Journal of Applied Engineering and Technological Science
Vol 4(1) 2022 : 451-459

FINITE ELEMENT ANALYSIS AND FABRICATION OF VORONOI PERFORATED WRIST HAND ORTHOSIS BASED ON REVERSE ENGINEERING MODELLING METHOD

Zakki Fuadi Emzain[1]*, Nanang Qosim[2], AM. Mufarrih[3], Syamsul Hadi[4]
Department of Mechanical Engineering, Politeknik Negeri Malang, Indonesia[1,2,3,4]
zfemzain@polinema.ac.id

Received : 06 November 2022, Revised: 08 December 2022, Accepted : 08 December 2022
**Corresponding Author*

ABSTRACT
Other than surgery, post-stroke spasticity, fractures due to accidents, sports injuries, and musculoskeletal disorders due to office work on the wrist can be treated using a wrist-hand orthosis. The customized conventional methods usually have some drawbacks, which are more expensive, take a long time to manufacture, and require expert skills from medical therapists. The presence of reverse engineering (RE) technology can be applied in the medical field, such as the manufacture of prosthetic or orthosis devices. This study aims to develop a reverse engineering-based wrist-hand orthosis design, analyze it using the finite element method, and fabricate it. Research methods included 3D scanning, CAD modelling, model analysis, 3D printing, and postprocessing. The model material used was PLA with variations in the thickness of 5 mm, 5.5 mm, and 6 mm, and the load values range from 0 N to 30 N. The results of the equivalent stress analysis showed that the 5 mm thickness model could withstand a load of 30 N with a maximum equivalent stress of 23.46 MPa. With a safety factor value of 2.56, it was still relatively safe, and a critical area was at the back end of the model's palm between the thumb and index finger. The equivalent elastic strain and deformation results also had the same graphic trend with the maximum values for the same model, which were 0.0076 mm and 0.614 mm, respectively. The 3D printing FDM result showed that the Voronoi perforated wrist-hand orthosis prototype was sturdy, fit, and comfortable. It is expected to hold muscle tone and immobilize for hand rehabilitation.

Keywords: *Finite Element Analysis; Reverse Engineering; Wrist-Hand Orthosis, Voronoi Perforated*

1. Introduction

The wrist is essential in daily activities such as lifting, pushing, and pulling objects. However, the wrist may not function optimally due to post-stroke spasticity, wrist fractures, and wrist injury. Wrist fractures can be caused by falls, accidents, and sports injuries (Hsu et al., 2021). Prolonged and inappropriate use of computers and mice can also cause musculoskeletal disorders. About 41% of diseases related to office work are musculoskeletal disorders in the upper extremities, including the neck, shoulders, arms, and wrists (Sirajudeen et al., 2018).

Treatment for spasticity, fracture, and injury to the wrist can be done with surgery if it is severe or with the use of wrist orthoses if it is relatively mild, depending on several factors (Calbiyik, 2018). An orthosis is an artificial device to hold or immobilize an injured patient's body part for recovery (Modi, 2018). The use of an orthosis also allows it to be used while doing activities or working while maintaining the fixed position of the body part. However, the orthosis sold generally is as uncomfortable as the customized one. Meanwhile, customized orthoses are more expensive, take a long time to manufacture, and require expert skills from medical therapists (Keller et al., 2021).

Generally, there are two methods for making conventional customized wrist-hand orthosis (WHO). The first method is with a plaster cast. The plaster cast is only used as a copy of the mould, which will then be used for orthosis models made of thermoplastic manually or by vacuum. The second method is to modify the thermoplastic, which is malleable after being softened with hot water directly on the patient's organs. However, both methods need to cut the unused thermoplastic parts outside the covered organ and add additions such as pads, glue, and plaster straps. This method also cannot be used for mass production and requires direct contact with the patient's organs (Palousek et al., 2014).

The use of wrist orthosis from 3D Printers has been proven to play a significant role as a substitute compared to conventional wrist orthosis from plaster, thermoplastic, and brace and has excellent prospects in the future (Zheng et al., 2020). Several previous studies related to the development of the manufacture of wrist orthosis have also been carried out by several researchers. A wrist orthosis model with a hybrid method has been developed, which combines the results of 3D printing as the inner layer and injection moulding as the outer layer with assembly principles such as plug-ins (H. Kim & Jeong, 2015). A hand orthosis using reverse engineering has been researched with a modified CAD model, such as a duck's foot with an additional surface between the fingers. The model is printed using FDM 3D Printing with ABS material with several small circular holes for ventilation under the palm to the wrist (Baronio et al., 2016).

Artificial wrist orthosis on patients has been tested with better results than using a wrist brace. The wrist orthosis design covers the wrist surface with a thickness of 1.8 mm and segmented holes in the carpometacarpal joint of the thumb and the top of the forearm. The material used is thermoplastic polyurethane (TPU) filament and is fabricated using a fused filament fabrication (FFF) 3D printer (S. J. Kim et al., 2018). A prototype wrist orthosis was made by combining two FDM printer materials: TPU for the inner layer and ABS for the outer layer. The model's design is divided into two parts, top, and bottom, for assembly using screws, and the ventilation holes are in the form of a parallelogram that is evenly distributed (Górski et al., 2019).

The manufacture of wrist splints has been developed using reverse engineering and in combination with finite element analysis. The research also tested the direction and angle of the printed material before fabricating the wrist splint using a 3D printer selective laser sintering (SLS) type (Modi & Khare, 2022). Although several studies have been related to the static wrist orthosis mentioned above, some prototype models of the wrist orthosis are still only at the bottom of the wrist and forearm. As a result, it is not covered all of the wrist areas. It should be better if the orthoses function could also be used as a protector from friction or impact on the top. While some dynamic wrist orthoses still look complicated in design and difficult to use (Ates et al., 2015; Sutton et al., 2016). So it is necessary to develop a static wrist orthosis that is more comfortable, sturdy, and easy to apply and wear.

The presence of reverse engineering (RE) and rapid prototyping (RP) technologies have been widely used, including in the medical field. Fabrication of tissues and organs, manufacture of prosthetics and orthoses/splints, implants, and anatomical models that can be modified are several forms of application in the medical field (Dodziuk, 2016). This benefit allows the creation of a suitable individual orthosis based on the patient's anthropometry (Young et al., 2019). The advantages of 3D printers are that they are easy to model, fast to manufacture, and cost-effective in production, making 3D printers very appropriate to be used as an alternative to orthoses (Choi et al., 2019). The use of finite element analysis can predict critical areas of a model so that the model design can be improved and refined before being fabricated (Qosim et al., 2020, 2022).

Therefore, further research is needed on the manufacture of wrist-hand orthosis using reverse engineering (RE) and rapid prototyping (RP) technology. This study aims to develop a wrist-hand orthosis model using a 3D Laser Scanner. Then the finite element analysis and fabrication of the model are carried out.

2. Research Methods

This study has four main steps, which are 3D scanning, CAD modelling, model analysis, and model fabrication. A flowchart of the stages of this research is shown in Figure 1 (Emzain et al., 2020). Firstly, the hand body of the patient was scanned from the fingers, palm, wrist, and forearm using EinScan-H 3D Scanner, where the specifications are suitable for scanning the human body. The hand object is required to remain motionless during the scanning time. The patient sits on a chair with an upright hand position using the elbow as a support on the table. Meanwhile, the scanner performer stands to scan around the object's hand using a 3D Scanner, and the laptop is on the table facing the scanner to determine the scanning progress. The arrangement of the object scanning flow can be seen in Figure 2.

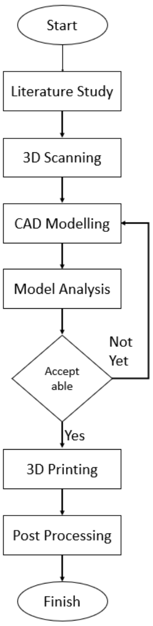

Fig. 1. Flowchart of research stages

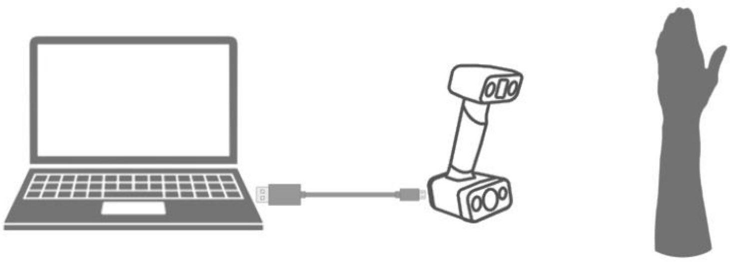

Fig. 2. Scan process settings

CAD modelling involves several steps: segmentation, thickening, venting, and making connections. These steps were conducted to create a design of the wrist-hand orthosis, which covers the wrist's surface, starting from the upper arm area to the tip of the palm. The analysis model stage was carried out to determine how much the maximum equivalent stress occurs and the specific location that experiences stress. Moreover, the result of the safety factor, equivalent elastic strain, and deformation was also covered in the analysis model.

Then, a fabrication model using fused deposition modelling (FDM) 3D Printing was used for prototyping the model. The most widely used plastic filament material, Polylactic Acid (PLA), was used as the primary material. PLA was chosen because it has a longer temperature resistance when the printing process is carried out with a long duration compared to Acrylonitrile Butadiene Styrene (ABS) material which is easy to wrap (Yang et al., 2021). The mechanical characteristics of PLA material can be seen in Table 1 (Jesus et al., 2022).

Table 1 - Mechanical characteristics of PLA material

Characteristics	Value	Unit
Density	1.24	g/cm^3
Young's Modulus	3100	MPa
Poisson's Ratio	0.39	
Yield Strength	60	MPa

3. Results and Discussions

3.1 3D Scanning

The scanned body part was made to exceed the core area of the wrist-hand orthosis model, which includes the fingers, palm, wrist, and forearm, so the segmentation process can be carried out efficiently. The configuration selected in the 3D scanning process included texture scan, high detail resolution with a point distance of 0.7 mm, watertight model, high detail meshing data, and 100% scaling ratio to obtain the best scanning result. Figure 3 shows the final file (.STL) resulting from 3D scanning.

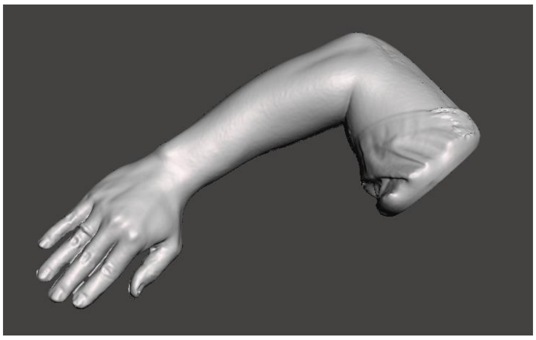

Fig. 3. 3D scanning result

3.2 CAD Modelling

In the model segmentation process, the finger and elbow areas were cut and removed at a certain distance and cutting angle. The remaining location boundaries were the forearm before the elbow until each finger's metacarpal tip area. Furthermore, the thickening process of the surface was made of 5 mm, 5.5 mm, and 6 mm. The configuration of accuracy was 50, and regularity was 50. Following this, the ventilation holes in the upper and lower model were made with the setting Dual Edge on Pattern Type and Tilling Mode Hex Grid. Then, an Element Dimension of 5 mm and Element Spacing of 0.2 mm were chosen to produce a medium-sized Voronoi diagram-shaped ventilation for the hand orthosis. The process of segmentation, thickening, and model hole-making is all done using Autodesk Meshmixer software. The result of making model ventilation holes is shown in Figure 4.

Fig. 4. Model with Voronoi perforated

The connection pattern was made like a puzzle, so the orthosis model will easily put on and take off. On the right side of the model, the puzzle pattern was made using an angle of approximately 135 degrees, while on the left side of the model, the puzzle pattern was made using an angle of roughly 45 degrees. The shape of the pattern that is made extends from the front end to the model's back end. The model connection was made using Autodesk Powershape Ultimate software. Figure 5 shows the final result of making the connection model. After that, the model will be converted from an STL file into a Solid Part before the model analysis process is carried out.

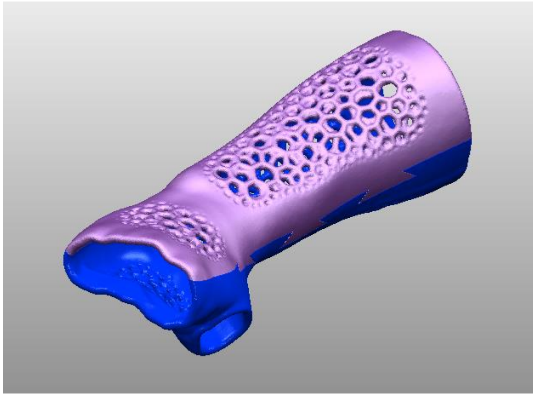
Fig. 5. The result of the connection model

3.3 Analysis Model

The meshing process was generated manually with an input element size of 2 mm, where the size produced a good-quality mesh. It can be seen that the majority of the mesh results are on a scale interval of 0.13 - 0.38 for quad4 and tri3-shaped elements. According to the Skewness scale, the closer to 0, the mesh quality is classified as good (Emzain et al., 2021). Figure 6 shows the results of the meshing model with mesh quality indicators. Boundary conditions for fixed support applied were on the top area of the model except for the ventilation holes starting from the back of the palm to the back of the arm. On the opposite side, especially in the area around the wrist to the tip of the palm, a force was applied with loading ranging from 0 to 30 N. This interval force is assumed to occur when the model is applied to the patient's hand for fixation. Figure 7 shows the boundary conditions of the wrist-hand orthosis model.

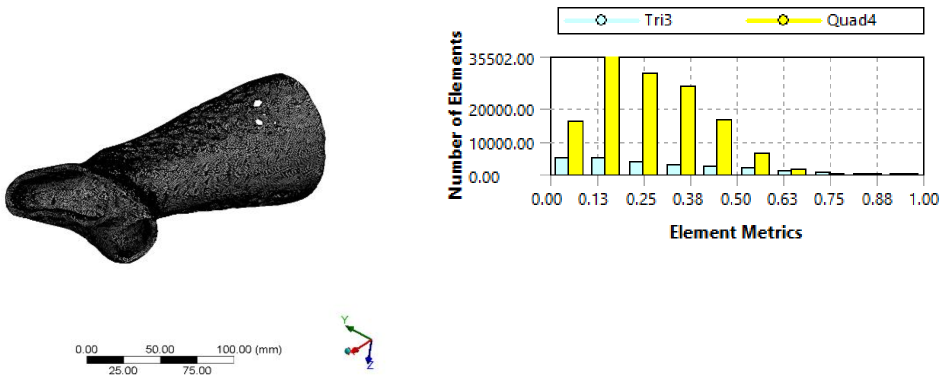

Fig. 6. Results of Meshing Models With Mesh Quality Indicators

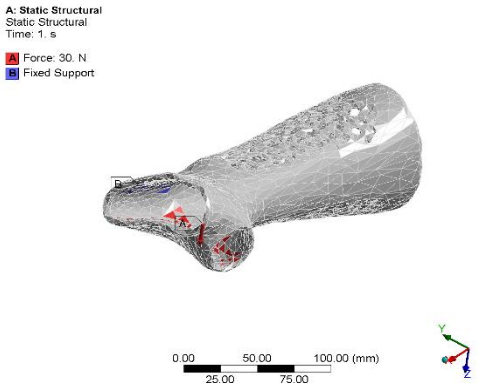

Fig. 7. Result of Boundary Condition Model

The analysis of the wrist-hand orthosis model for the equivalent (von Mises) stress showed that the maximum stress occurred in the area of the back end of the model's hand. This area is the link between the thumb and index finger, where the two fingers have a greater force than the other. Figure 8 shows the results of equivalent stress by indicating the maximum stress area and a graph of the relationship between load and stress from variations in the model's thickness. The maximum stress in the most significant load of 30 N was experienced in the model size of 5 mm, which was 23.46 MPa. This value is considered safe because it is still far below the Tensile Strength value of the PLA material. By calculation using the safety factor formula as follows.

$$n = \frac{\sigma_{\text{yield}}}{\sigma_{\text{actual}}}$$

Therefore, the maximum stress in the model has a safety factor of 2.56.

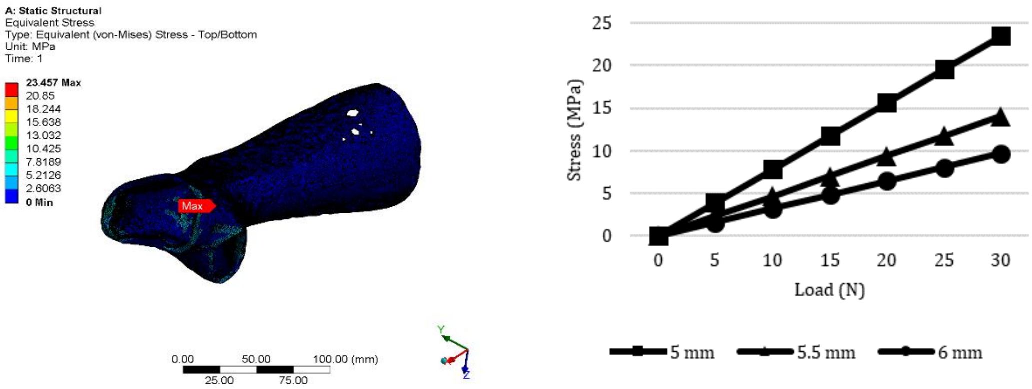

Fig. 8. The Results of The Equivalent Stress Model and The Graph of The Relationship Between Load and Stress From Variations in Model Thickness

Meanwhile, the wrist hand orthosis model from the equivalent elastic strain also showed the same trend, and the maximum strain area was the same as the equivalent stress for the three types of model thickness. The maximum strain value with the most significant load of 30 N was found in the 5 mm thickness model, 0.0076 mm. The strain value is well received because the value is still relatively small. While the 6 mm thickness model was the smallest, the maximum strain value was 0.0032. Figure 9 shows the results of the equivalent elastic strain with the indication of the maximum strain area and a graph of the load-strain relationship from the variation in the model's thickness.

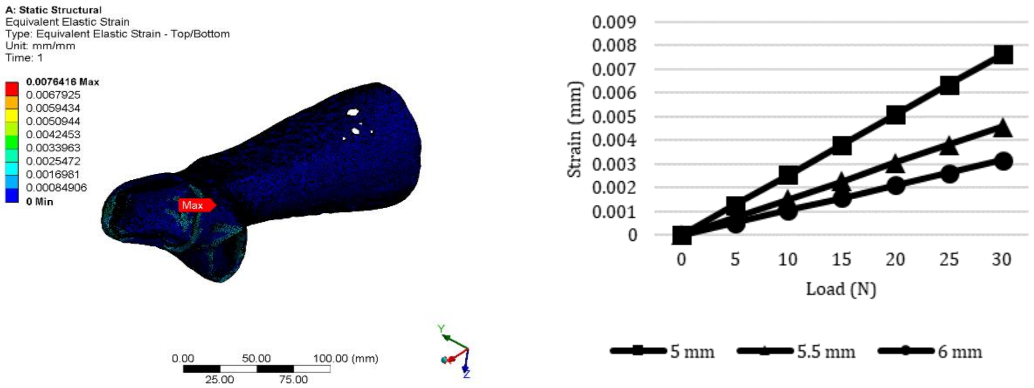

Fig. 9. The Results of The Equivalent Elastic Strain Model and The Graph of The Relationship Between Load and Strain From Variations in The Thickness of The Model

On top of that, the deformation result of the wrist-hand orthosis model analysis showed that the area of the palm end of the model experienced the most significant deformation. It is reasonable and can occur because the area is the border of the palm with the fingers, where the hand's position tends to be bent as the center of the load. The most considerable deformation value occurred in the 5 mm thickness model, 0.614 mm, while the smallest deformation value occurred in the 6 mm model, 0.172 mm. Figure 10 shows the deformation results with the indication of the maximum deformation area and a graph of the relationship between load and deformation from variations in the model's thickness.

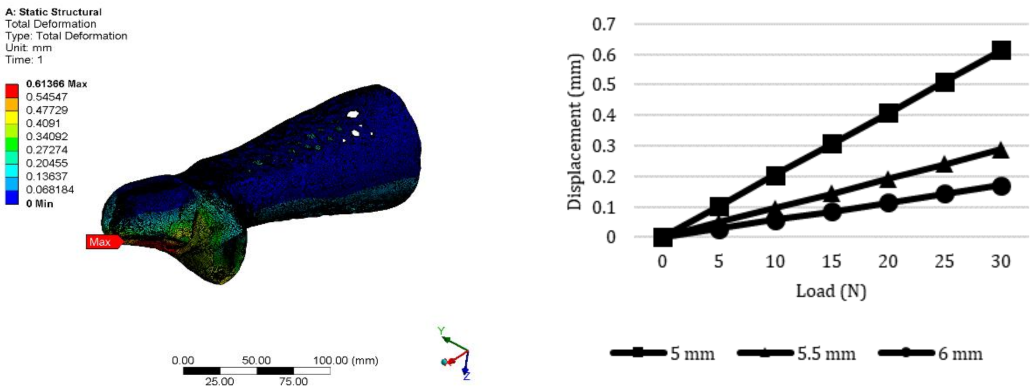

Fig. 10. The Results of The Deformation Model and The Graph of The Relationship Between Load and Deformation From Variations in The Thickness of The Model

3.4 Model Fabrication

The wrist-hand orthosis model using Polylactic Acid (PLA) material was fabricated separately between the lower and upper parts using the 3D Printing Fused Deposition Modeling (FDM). The parameters used were nozzle size 0.4 mm, layer height 0.2 mm, shell thickness 0.8 mm, infill density 80%, material printing temperature 208 °C, and printing speed 50 mm/s. The 3D printing FDM prototype results showed that both parts were successfully printed and assembled. With a thickness of 5 mm, the prototype model felt sturdy due to the high infill density, even though it results in a longer printing time. The model's shape was very fit and comfortable when worn because the inner surface of the model was smooth, and the general support was placed on the outer surface. With the strength of the model, the model is certainly able to withstand muscle tone for stroke sufferers and the load of the wrist and palm for hand rehabilitation fixation. The use of the model on the hand can be seen in Figure 11.

Fig. 11. Wearing The Wrist Hand Orthosis Model on The Hand

5. Conclusion

The design of the Voronoi perforated wrist hand orthosis model that has a shape like the surface of a human hand has been successfully created using the reverse engineering modelling method. Reverse engineering modelling started with scanning objects using a 3D scanner, then in 3D modelling, involved the segmentation process, thickening, venting, making connections, and converting model formats. Furthermore, the model design was analyzed using the finite element method with variations in thickness and loading. The analysis model results showed that the maximum equivalent stress occurred in the 5 mm thickness model with a maximum stress of 23.46 MPa, which is classified as safe with a safety factor of 2.56. The area that experienced maximum equivalent stress occurred in the back of the model's palm between the thumb and index finger. The results of the equivalent elastic strain also have the same graph trend and the same maximum area, with the maximum strain value found in the 5 mm thickness model, which was 0.0076 mm, which is still relatively small. While the deformation results showed that the palm end area of the model experienced the most considerable deformation, and the maximum deformation occurred in the 5 mm thickness model, which was 0.614 mm. The model fabrication result showed that the wrist-hand orthosis prototype is sturdy, fit in shape, and comfortable. The model can withstand muscle tone for stroke sufferers and the load of the wrist and palm for hand rehabilitation fixation.

Acknowledgement - optional

We want to express our gratitude to the UPT 2M Politeknik Negeri Malang, which has funded this research with SP DIPA– 023.18.2.677606/2022.

References

Ates, S., Mora-Moreno, I., Wessels, M., & Stienen, A. H. A. (2015). Combined active wrist and hand orthosis for home use: Lessons learned. *2015 IEEE International Conference on Rehabilitation Robotics (ICORR)*, 398–403.

Baronio, G., Harran, S., & Signoroni, A. (2016). A critical analysis of a hand orthosis reverse engineering and 3D printing process. *Applied Bionics and Biomechanics*, *2016*.

Calbiyik, M. (2018). Fixation of unstable distal radius fractures by using expandable Intramedullary nailing system in adult patients. *Pakistan Journal of Medical Sciences*, *34*(1), 198.

Choi, H., Seo, A., & Lee, J. (2019). Mallet Finger Lattice Casts Using 3D Printing. *Journal of Healthcare Engineering*, *2019*.

Dodziuk, H. (2016). Applications of 3D printing in healthcare. *Kardiochirurgia i Torakochirurgia Polska= Polish Journal of Cardio-Thoracic Surgery*, *13*(3), 283.

Emzain, Z. F., Amrullah, U. S., Mufarrih, A., Qosim, N., & Herlambang, Y. D. (2021). Design optimization of sleeve finger splint model using Finite Element Analysis. *Jurnal Polimesin*, *19*(2), 147–152.

Emzain, Z. F., Huang, S.-C., Yang, Y.-S., & Qosim, N. (2020). Design and Analysis of a Dynamic Splint Based on Pulley Rotation for Post-Stroke Finger Extension Rehabilitation Device. *Rekayasa Mesin*, *11*(3), 477–485.

Górski, F., Kuczko, W., Weiss, W., Wichniarek, R., & Żukowska, M. (2019). Prototyping of an Individualized Multi-Material Wrist Orthosis using Fused Deposition Modelling. *Advances* *in Science and Technology. Research Journal*, *13*(4).

Hsu, H., Fahrenkopf, M. P., & Nallamothu, S. V. (2021). Wrist fracture. *StatPearls [Internet]*.

Jesus, L. C. C., Oliveira, J. M., Leão, R. M., Beltrami, L. R., Zattera, A. J., Anflor, C. T. M., Doca, T. C. R., & Luz, S. M. (2022). Tensile behavior analysis combined with digital image correlation and mechanical and thermal properties of microfibrillated cellulose fiber/polylactic acid composites. *Polymer Testing*, 107665.

Keller, J. L., Henderson, J. P., Landrieu, K. W., Dimick, M. P., & Walsh, J. M. (2021). The 2019 practice analysis of hand therapy and the use of orthoses by certified hand therapists. *Journal of Hand Therapy*.

Kim, H., & Jeong, S. (2015). Case study: Hybrid model for the customized wrist orthosis using 3D printing. *Journal of Mechanical Science and Technology*, *29*(12), 5151–5156.

Kim, S. J., Kim, S. J., Cha, Y. H., Lee, K. H., & Kwon, J.-Y. (2018). Effect of personalized wrist orthosis for wrist pain with three-dimensional scanning and printing technique: a preliminary, randomized, controlled, open-label study. *Prosthetics and Orthotics International*, *42*(6), 636–643.

Modi, Y. K. (2018). Calcium sulphate based 3D printed tooling for vacuum forming of medical devices: an experimental evaluation. *Materials Technology*, *33*(10), 642–650.

Modi, Y. K., & Khare, N. (2022). Patient-specific polyamide wrist splint using reverse engineering and selective laser sintering. *Materials Technology*, *37*(2), 71–78.

Palousek, D., Rosicky, J., Koutny, D., Stoklásek, P., & Navrat, T. (2014). Pilot study of the wrist orthosis design process. *Rapid Prototyping Journal*.

Qosim, N., Emzain, Z. F., Mufarrih, A. M., Monasari, R., Kusumattaqiin, F., & Santoso, R. E. (2022). Finite Element Analysis of SS316L-Based Five-Hole Plate Implant For Fibula Reconstruction. *Journal of Applied Engineering and Technological Science (JAETS)*, *4*(1), 16–23.

Qosim, N., Monasari, R., Emzain, Z. F., Hakim, L., & Sai'in, A. (2020). Finite Element Analysis of Miniplate for Post-Fracture Finger Rehabilitation Device. *Journal of Applied Engineering and Technological Science (JAETS)*, *2*(1), 21–26.

Sirajudeen, M. S., Alaidarous, M., Waly, M., & Alqahtani, M. (2018). Work-related musculoskeletal disorders among faculty members of college of Applied Medical Sciences, Majmaah University, Saudi Arabia: A cross-sectional study. *International Journal of Health Sciences*, *12*(4), 18.

Sutton, L., Moein, H., Rafiee, A., Madden, J. D. W., & Menon, C. (2016). Design of an assistive wrist orthosis using conductive nylon actuators. *2016 6th IEEE International Conference on Biomedical Robotics and Biomechatronics (BioRob)*, 1074–1079.

Yang, Y.-S., Emzain, Z. F., & Huang, S.-C. (2021). Biomechanical Evaluation of Dynamic Splint Based on Pulley Rotation Design for Management of Hand Spasticity. *IEEE Transactions on Neural Systems and Rehabilitation Engineering*, *29*, 683–689.

Young, K. J., Pierce, J. E., & Zuniga, J. M. (2019). Assessment of body-powered 3D printed partial finger prostheses: a case study. *3D Printing in Medicine*, *5*(1), 1–8.

Zheng, Y., Liu, G., Yu, L., Wang, Y., Fang, Y., Shen, Y., Huang, X., Qiao, L., Yang, J., & Zhang, Y. (2020). Effects of a 3D-printed orthosis compared to a low-temperature thermoplastic plate orthosis on wrist flexor spasticity in chronic hemiparetic stroke patients: a randomized controlled trial. *Clinical Rehabilitation*, *34*(2), 194–204.